

Contrastive Prompt Clustering for Weakly Supervised Semantic Segmentation

Wangyu Wu^{a,b}, Zhenhong Chen^c, Xiaowen Ma^d, Wenqiao Zhang^d, Xianglin Qiu^{a,b}, Siqu Song^{a,b}, Xiaowei Huang^b, Fei Ma^{a,*}, Jimin Xiao^{a,*}

^a*Xi'an Jiaotong-Liverpool University, Suzhou, China*

^b*University of Liverpool, Liverpool, UK*

^c*Microsoft, Redmond, USA*

^d*Zhejiang University, Hangzhou, China*

Abstract

Weakly Supervised Semantic Segmentation (WSSS) with image-level labels has gained attention for its cost-effectiveness. Most existing methods emphasize inter-class separation, often neglecting the shared semantics among related categories and lacking fine-grained discrimination. To address this, we propose Contrastive Prompt Clustering (CPC), a novel WSSS framework. CPC exploits Large Language Models (LLMs) to derive category clusters that encode intrinsic inter-class relationships, and further introduces a class-aware patch-level contrastive loss to enforce intra-class consistency and inter-class separation. This hierarchical design leverages clusters as coarse-grained semantic priors while preserving fine-grained boundaries, thereby reducing confusion among visually similar categories. Experiments on PASCAL VOC 2012 and MS COCO 2014 demonstrate that CPC surpasses existing state-of-the-art methods in WSSS.

Keywords: Weakly-Supervised Learning, Semantic Segmentation, Large Language Model, Contrastive Learning

*Corresponding authors

Email addresses: wangyu.wu@liverpool.ac.uk (Wangyu Wu), zcheh@microsoft.com (Zhenhong Chen), xwma@zju.edu.cn (Xiaowen Ma), wenqiaozhang@zju.edu.cn (Wenqiao Zhang), Xianglin.Qiu20@student.xjtlu.edu.cn (Xianglin Qiu), Siqu.Song22@student.xjtlu.edu.cn (Siqu Song), xiaowei.huang@liverpool.ac.uk (Xiaowei Huang), fei.ma@xjtlu.edu.cn (Fei Ma), jimin.xiao@xjtlu.edu.cn (Jimin Xiao)

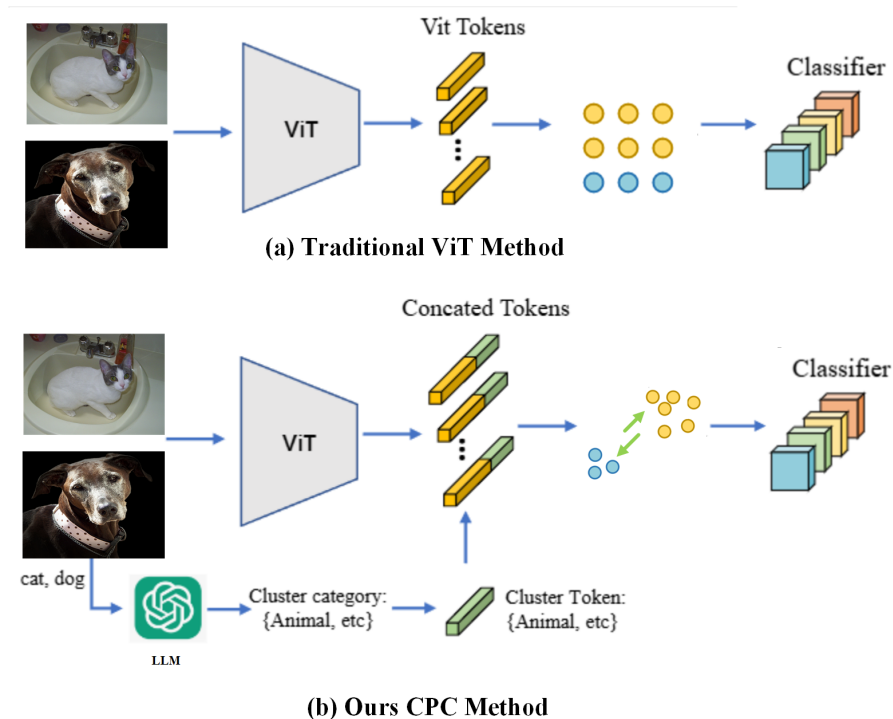


Figure 1: (a) In traditional ViT-based WSSS methods, only the ViT tokens representing image patches are used for classification. (b) In our CPC, we leverage a Large Language Model (LLM) to determine the cluster category of each image and generate a cluster token that encodes shared class information. This cluster token, combined with contrastive learning, enhances the ViT patch tokens.

1. Introduction

Weakly supervised semantic segmentation (WSSS) utilizes image-level labels to achieve dense pixel-level predictions Wu et al. (2025b, 2024a). In particular, WSSS refers to methods that rely solely on image-level annotations instead of detailed pixel-level labels. This approach significantly reduces the annotation cost and effort, while still producing high-resolution segmentation maps in which each pixel is assigned a semantic label.

Recently, many WSSS methods Kweon & Yoon (2024); Yin et al. (2023); Chen et al. (2024); Li et al. (2023) adopt the Vision Transformer (ViT) architec-

ture Dosovitskiy et al. (2020); Xue et al. (2025); Wu et al. (2024b), due to its capability to capture global contextual dependencies through self-attention mechanisms. These mechanisms allow ViT to model long-range interactions across an image, thereby improving semantic coherence. However, the self-attention in ViT also tends to act as a low-pass filter, diminishing the variance of local features and leading to excessive smoothing Yin et al. (2024). This effect often suppresses high-frequency details that are critical for preserving fine-grained boundaries and intra-object distinctions, which ultimately weakens the discriminability of patch-level features and harms segmentation quality. In addition, existing WSSS approaches Li et al. (2024); Yin et al. (2024); Guo et al. (2024) typically emphasize maximizing inter-class separation to reduce class confusion. While this strategy can enhance overall discriminative power, it often overlooks the valuable shared semantic information among visually or semantically similar categories. We argue that mining and leveraging such shared information is essential for capturing the latent structure of the semantic space. To this end, we propose to group related classes into semantic clusters, and inject their shared features into patch representations to mitigate the over-smoothing effect and reduce ambiguity, as illustrated in Fig. 1.

To effectively identify and exploit these inter-category relationships, we introduce an approach called **Contrastive Prompt Clustering (CPC)**. Our method leverages the capabilities of Large Language Models (LLMs) to automatically generate prompts that encode semantic affinities between categories, enabling the construction of prompt-guided clusters. These clusters serve as a form of high-level relational prior, guiding the network to recognize shared information across similar classes.

Furthermore, to strengthen class-level discriminability, we introduce a class-aware contrastive learning module that operates at the patch level. This module enforces intra-class compactness and inter-class separability by pulling embeddings from the same class closer together and pushing embeddings from different classes farther apart. Unlike prompt clustering, which models coarse-grained semantic similarities, the contrastive objective imposes fine-grained visual con-

straints, even for classes that belong to the same semantic cluster. This hierarchical design enables the model to benefit from both shared semantic priors and class-specific visual distinctions.

Our main contributions are fourfold:

- We propose a ViT-based WSSS framework that integrates prompt-derived category clusters and class labels into the segmentation process, enriching the model’s semantic representation.
- We develop an automated semantic clustering method based on GPT-generated prompts, enabling the model to discover and utilize inter-category relationships without external supervision.
- We introduce a class-aware patch-level contrastive learning objective that enhances fine-grained class discrimination while remaining compatible with the prompt-guided clustering strategy.
- We demonstrate the effectiveness of our approach on both the PASCAL VOC 2012 and MS COCO 2014 datasets, where our method achieves superior performance compared to state-of-the-art WSSS methods.

In summary, the proposed CPC framework presents a unified strategy that combines language-derived semantic clustering with contrastive visual discrimination. Our work highlights the synergy between prompt-driven knowledge and contrastive representation learning, offering a new perspective on bridging vision-language priors and fine-grained segmentation in weakly supervised settings.

2. Related Work

2.1. WSSS with Image-level Labels

Weakly Supervised Semantic Segmentation (WSSS) with image-level labels generally begins by generating pseudo labels using CAM Wu et al. (2024c, 2025a); Zhang et al. (2025); Wu et al. (2025c). However, since CAMs tend to highlight

only the most discriminative regions of an object, numerous methods have been developed to overcome this limitation. For instance, techniques such as erasing Wei et al. (2017); Jiang et al. (2022), online attention accumulation Jiang et al. (2019), and cross-image semantic mining Sun et al. (2020) have been proposed to broaden the activated regions. Additional works Lee et al. (2021); Yao et al. (2021) employ supplementary saliency maps to both suppress background interference and identify non-salient object parts. Other approaches Chen et al. (2022); Du et al. (2022); Cao & Zhang (2023); Yaganapu & Kang (2024); Xu et al. (2019); Luo et al. (2022) leverage contrasts between pixel and prototype representations to encourage more complete object activation. Furthermore, the method in Chang et al. (2020) enhances the segmentation process by integrating extra category information or by refining the learned representations through additional information mining on the training data. Recent advances have also seen the adoption of ViT for WSSS. Models such as MCTformer Xu et al. (2022) and AFA Ru et al. (2022) use ViT’s attention mechanisms to generate localization maps and produce pseudo labels via PSA Ahn & Kwak (2018), and AFA through a combination of multi-head self-attention and an affinity module. Meanwhile, ViT-PCM Rossetti et al. (2022) explores a CAM-independent approach by utilizing patch embeddings and max pooling to estimate pixel-level label probabilities, albeit with the risk of patch misclassification. In contrast to these strategies, our proposed CPC exploits additional cluster information to further enhance the segmentation performance of WSSS by improving its ability to distinguish between different classes.

2.2. Vision Transformers for WSSS

ViTDosovitskiy et al. (2020) has achieved impressive results across a range of vision tasksXie et al. (2024b); Xu et al. (2019); Luo et al. (2022); Liu et al. (2025, 2024); Xie et al. (2024a); Dosovitskiy et al. (2020). This success has naturally led to the integration of ViT into WSSS, where ViT-based approaches are emerging as viable alternatives to traditional CNN-based methods for generating CAMXu et al. (2022); Ru et al. (2022). For example, MCTformer Xu et al. (2022) utilizes

the inherent attention mechanisms of ViT to derive localization maps and employs PSA Ahn & Kwak (2018) for pseudo mask generation. Similarly, AFA Ru et al. (2022) capitalizes on ViT’s multi-head self-attention to capture global context and uses an affinity module to propagate pseudo masks. Despite these advances, the challenge of over-smoothing inherent in ViT remains a significant hurdle. ViT-PCM Rossetti et al. (2022) attempts to address this by abandoning CAM in favor of a method based on patch embeddings combined with max pooling to infer pixel-level label probabilities, although this may introduce errors when patches are misclassified. Our approach sets itself apart by incorporating additional cluster information to augment the WSSS framework’s capacity to recognize and differentiate among various classes, thereby addressing some of the limitations present in existing ViT-based methods.

2.3. Prompt-based Language Models

Prompt-based learning improves the performance of pre-trained language models (PLMs) by incorporating task-specific instructions into the input. Early methods relied on manually designed prompts to adapt to various generation tasks Brown et al. (2020); Raffel et al. (2020); Zou et al. (2021); Chen et al.; Fang et al. (2025); Jin et al. (2025). However, these handcrafted prompts lack the flexibility to be easily applied to new tasks. As a result, recent advancements have focused on automating prompt generation Shin et al. (2020). Additionally, some approaches Liu et al. (2023); Li & Liang (2021) have explored optimizing continuous prompts to address the challenges posed by optimizing discrete prompts, offering improved flexibility across different tasks. More recently, PLMs have been applied to computer vision tasks, with one method Zhang et al. (2023) utilizing prompts to enhance few-shot learning. In contrast, our approach leverages PLMs to generate prompts that enhance the diversity of image description text. To the best of our knowledge, this is the first time PLMs have been used to generate cluster information to improve the WSSS task.

3. Methodology

In this section, we present the overall architecture and key components of our proposed Contrastive Prompt Clustering framework. We begin in Sec. 3.1 with a high-level overview of the entire pipeline, including its core structures and interactions. Then, in Sec. 3.2, we introduce our prompt-driven category clustering method, which leverages the powerful semantic reasoning capability of Large Language Models (LLMs) to automatically group semantically similar categories. These clusters enable the model to better model inter-class relationships and reduce semantic confusion. In Sec. 3.3, we describe how the clustered category tokens are integrated into the ViT backbone to enhance semantic discrimination.

Finally, in Sec. 3.4, we introduce a class-aware patch contrastive learning objective that reinforces intra-class consistency by pulling together high-confidence patch embeddings from the same class while pushing away low-confidence ones. This component complements prompt-based clustering by aligning local visual features with semantic category coherence.

3.1. Overall Framework

As illustrated in Fig. 2, we provide a comprehensive overview of our proposed **CPC** framework. The network is designed to predict patch-level semantic labels by injecting both visual features and semantic cluster priors into the representation learning process. Specifically, the original ViT patch tokens are concatenated with a set of cluster tokens derived from LLM-guided prompt clustering, resulting in enriched patch representations. These tokens are further refined using a HV-BiLSTM module Rossetti et al. (2022) to better model inter-patch dependencies.

A lightweight MLP-based classifier then predicts the patch-to-category associations, generating coarse pseudo-labels. These initial predictions are post-processed with a Conditional Random Field (CRF) Krähenbühl & Koltun (2011) to enforce spatial consistency and semantic alignment, resulting in high-quality pseudo-labels.

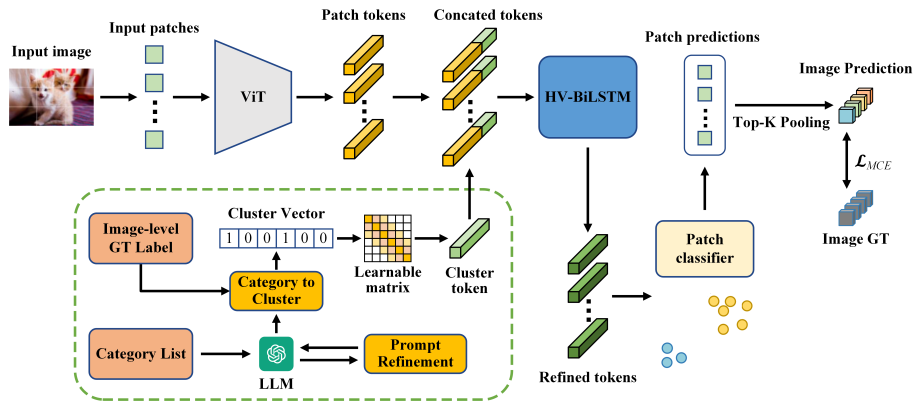


Figure 2: The overall framework of our proposed CPC is illustrated. First, a ViT backbone is used to extract patch-level tokens from the input image. Meanwhile, a predefined category list is fed into LLM to generate clusters of semantically related categories. Based on the image-level labels, a binary cluster vector is constructed, where 1 indicates membership in a cluster and 0 otherwise. This vector is multiplied with a learnable projection matrix to produce a cluster token that encodes semantic cluster information. The cluster token is then concatenated with the patch tokens and fed into a HV-BiLSTM module to produce refined patch embeddings. These embeddings are used in two branches: (1) a patch classifier outputs patch-level class probabilities, which are aggregated via top-k pooling to obtain image-level predictions for computing the MCE loss; (2) a patch contrastive learning module enhances intra-class consistency by pulling together confident patches of the same class and pushing them away from uncertain patches. The final pseudo-labels are generated via CRF post-processing and used to train a segmentation network.

In parallel, we apply a patch contrastive loss on the intermediate feature space to enforce intra-class compactness and improve the robustness of patch-level representations (see Sec. 3.4). This contrastive module operates on confident patch pairs, promoting more discriminative and stable embeddings.

Finally, the refined pseudo-labels are used to train a DeepLabv2 Chen et al. (2018) segmentation network in a fully supervised manner, which produces the final dense semantic predictions. This two-stage training pipeline enables our framework to effectively leverage both language-guided clustering and feature-level supervision, achieving superior performance in weakly supervised semantic segmentation.

Algorithm 1: Self-Refine category clusters generation

Input : category list l , LLM \mathcal{M} , initial prompt p_{gen} , refine prompt p_{refine} , stop condition $s()$, number of queries R

Output: category clusters z_t

```
1 // Step 1: Multi-query initialization with voting
2 Initialize result set  $\mathcal{Z} = \{\}$ 
3 for  $r = 1$  to  $R$  do
4    $z^{(r)} = \mathcal{M}(p_{\text{gen}} \parallel l)$  with  $T=0$ ;
5    $\mathcal{Z} = \mathcal{Z} \cup \{z^{(r)}\}$ ;
6  $z_0 =$  most frequent element in  $\mathcal{Z}$ ;
7 // Step 2: Iterative refinement for iteration  $t \in \{0, 1, \dots\}$  do
8    $z_{t+1} = \mathcal{M}(p_{\text{refine}} \parallel z_t)$ ;
9   if  $s(z_{t+1}, z_t, \dots, z_0)$  then
10    break;
11 return  $z_t$ ;
```

3.2. Self-Refine Prompt for Cluster

The motivation behind clustering categories arises from our observation that, in previous works, models are typically designed to maximize the distance between different classes while minimizing the distance within the same class. This approach often leads to the assumption that the distances between all classes are equidistant, ignoring their intrinsic semantic similarities. For instance, a model might perceive the distance from “cat” to “dog” as equal to the distance from “cat” to “car,” despite the fact that “cat” and “dog” share significantly more similarities as animals, whereas “cat” and “car” are entirely distinct objects. To address this limitation and better capture the nuanced relationships between classes, we propose to abstract more granular cluster information at the class level. Specifically, we harness the powerful capabilities of LLMs to assign distinct cluster tags to these classes. However, due to the inherent instability of LLMs Madaan et al. (2024), the generated cluster tags may lack sufficient reliability.

To mitigate this issue and enhance robustness, we query the LLM R times using a fixed prompt schema and temperature $T=0$, generating R candidate cluster partitions for the category list. We then perform frequency-based voting across these partitions and select the most commonly occurring cluster configuration as the final result. The number of clusters is determined by the majority count observed across all queries, enabling a data-driven estimation of cluster granularity.

We integrate this self-refining prompt method into our clustering pipeline, as elaborated in Algo. 1 and visually represented by the Category Cluster module in Fig. 2. Here, R denotes the number of repeated LLM queries for initialization, \mathcal{Z} represents the set of all sampled cluster results $z^{(r)}$, and the function `most_frequent(\cdot)` selects the most commonly occurring configuration among them. These partitions are generated under deterministic decoding ($T=0$) and aggregated via majority voting to identify the most stable clustering outcome.

The clustering generation process is thus transformed into a consensus-

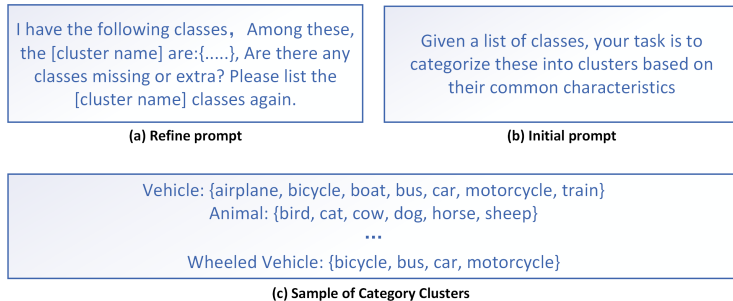


Figure 3: The proposed Prompt strategy.(a) is the refined prompt template; (b) is the initial prompt template; (c) is the samples of category clusters.

driven mechanism, where the initial phase collects candidate partitions via multiple deterministic LLM queries. Starting with a comprehensive category list l extracted from the dataset, we initially utilize a clustering prompt p_{gen} (depicted in Fig. 3(b)) in conjunction with GPT-4o (\mathcal{M}) to generate preliminary category clusters. This phase lays the groundwork by establishing baseline associations between semantic concepts.

Following this, the algorithm enters an optimization loop, where a refinement prompt p_{refine} (illustrated in Fig. 3(a)) facilitates iterative enhancements. At each iteration t , the language model \mathcal{M} processes the current cluster configuration z_t through the refinement template to produce an improved version z_{t+1} . The stopping condition $s()$ evaluates convergence by monitoring cluster stability across three consecutive iterations (i.e., when $z_{t+1} = z_t = z_{t-1}$), ensuring that the algorithm terminates only when the semantic groupings reach a stable equilibrium. This mechanism guarantees that the final clusters are both semantically coherent and robust.

Through this iterative generation-refinement process, the method systematically consolidates semantically coherent clusters, progressively enhancing their accuracy and consistency. Fig. 3(c) illustrates final cluster samples that exhibit significantly improved categorical cohesion compared to the initial groupings, highlighting the effectiveness of the refinement mechanism. The dynamic nature of this process enables the system to refine semantic relationships through suc-

cessive reasoning steps, ultimately yielding more precise and meaningful cluster configurations.

3.3. Category Cluster Tokens for WSSS

To enhance the richness of category information, we integrate cluster tokens as supplementary components within the training framework. These tokens enable the network to more effectively capture and utilize similarity relationships across diverse categories. Specifically, we concatenate ViT tokens with cluster tokens to construct the final input tokens, thereby optimizing the model’s capacity to leverage inter-class similarities. For example, while the label “car” represents a distinct category, the label “cat” exhibits greater similarity to “dog” due to shared semantic attributes. Consequently, both “cat” and “dog” are grouped into clusters such as “animal” or “pet,” reflecting their common contextual characteristics and enabling the model to better understand and exploit these relationships during training.

The pipeline of our proposed method is depicted in Fig. 2. The input image X , with dimensions $\mathbb{R}^{h \times w \times 3}$, is fed into a Vision Transformer (ViT) encoder to extract patch tokens $F_v \in \mathbb{R}^{s \times e}$, where $s = (n/d)^2$ denotes the number of tokens and e represents the dimensionality of each token. In practice, all input images are resized to consistent dimensions h and w , such that $n = h = w$, and d corresponds to the patch size. To incorporate cluster-level information, we design a cluster vector $u \in \mathbb{R}^L$ to indicate the cluster affiliations of X . Each element $u_i \in \{0, 1\}$ signifies the presence (1) or absence (0) of cluster category i , where L represents the total number of category clusters. This cluster vector u is then mapped to a cluster token $F_c \in \mathbb{R}^H$ through a learnable matrix $G \in \mathbb{R}^{L \times H}$, computed as follows:

$$F_c = u^T \cdot G. \tag{1}$$

Subsequently, we concatenate the cluster token F_c with each patch token, resulting in the combined tokens $F_{in} \in \mathbb{R}^{s \times (e+H)}$. This integration enables the

WSSS framework to more effectively perceive and utilize cluster-level information, thereby significantly enhancing the overall segmentation performance by leveraging the enriched contextual relationships between categories.

We employ a HV-BiLSTM module to refine the concatenated tokens F_{in} , producing refined tokens $F_{out} \in \mathbb{R}^{s \times (e+H)}$ with identical dimensions. Following this refinement, we introduce a one-layer Multi-Layer Perceptron (MLP) patch classifier, parameterized by a weight matrix $W \in \mathbb{R}^{(e+H) \times C}$, where C denotes the total number of classes. By applying the MLP and SoftMax operations, we generate predictions $Z \in \mathbb{R}^{s \times C}$ from the patch classifier, formulated as follows:

$$Z = \text{softmax}(F_{out}W), \quad (2)$$

the variable Z represents the patch-level predictions for semantic segmentation. To align these patch predictions with the image-level supervision required for training, it is necessary to transform them into image class predictions. This conversion is essential for accurate loss computation and ensuring that the predictions are consistent with the provided image-level labels. To achieve this, we employ a Top-K pooling mechanism to aggregate the patch predictions and derive the image class predictions p_c for class c , as follows:

$$p_c = \frac{1}{k} \sum_{i=1}^k \text{Top-k}(Z_j^c) \quad \text{and} \quad j \in \{1, \dots, s\}, \quad (3)$$

where $\text{Top-k}(\cdot)$ denotes the operation of selecting the top k patches with the highest prediction values for class c . This mechanism ensures that the final image-level predictions are robust and not disproportionately influenced by any anomalous or outlier patches.

3.4. Patch Contrastive Learning for Intra-Class Consistency

While the proposed Prompt-guided Clustering module effectively captures inter-class semantic relationships, it remains crucial to enhance the consistency of patch embeddings within each class to ensure robust predictions. To address this, we introduce a Patch Contrastive Error (PCE) loss, which explicitly pulls

together high-confidence patch embeddings of the same class while simultaneously pushing them away from low-confidence embeddings within that class.

Let F_{out} denote the refined patch embeddings and Z denote the patch prediction scores from the MLP classifier. For a given category c , we define high-confidence patches as $\mathcal{P}_{high}^c = \{F_{out}^i \mid Z_i^c > \epsilon\}$ and low-confidence patches as $\mathcal{P}_{low}^c = \{F_{out}^i \mid Z_i^c < 1 - \epsilon\}$, where ϵ is a predefined confidence threshold.

We measure similarity between two embeddings using cosine similarity:

$$S(F_{out}^i, F_{out}^j) = \frac{F_{out}^i \cdot F_{out}^j}{\|F_{out}^i\| \|F_{out}^j\|}, \quad (4)$$

which is normalized to $[0, 1]$ by:

$$\bar{S}(F_{out}^i, F_{out}^j) = \frac{1 + S(F_{out}^i, F_{out}^j)}{2}. \quad (5)$$

The overall Patch Contrastive Error for category c is then formulated as:

$$\begin{aligned} \mathcal{L}_{PCE}^c = & \frac{1}{N_{pair}^+} \sum_{i=1}^{|\mathcal{P}_{high}^c|} \sum_{j=1, j \neq i}^{|\mathcal{P}_{high}^c|} (1 - \bar{S}(F_{high}^i, F_{high}^j)) \\ & + \frac{1}{N_{pair}^-} \sum_{m=1}^{|\mathcal{P}_{high}^c|} \sum_{n=1}^{|\mathcal{P}_{low}^c|} \bar{S}(F_{high}^m, F_{low}^n), \end{aligned} \quad (6)$$

where N_{pair}^+ and N_{pair}^- denote the number of high-high and high-low patch pairs, respectively. The first term minimizes intra-class embedding variance, while the second term penalizes similarity between confident and uncertain regions, effectively pushing them apart.

By incorporating this class-aware contrastive learning module, the model benefits from both global semantic alignment via CPC and local feature consistency within each class, resulting in more accurate and coherent segmentation outcomes.

3.5. Overall Loss

We minimize the multi-label classification prediction error (MCE) between the predicted image-level labels p_c and the ground truth image labels y_c , ensuring

that the model’s predictions align closely with the actual annotations. This optimization process is formalized as follows:

$$\begin{aligned}\mathcal{L}_{MCE} &= \frac{1}{C} \sum_{c \in \mathcal{C}} BCE(y_c, p_c) \\ &= -\frac{1}{C} \sum_{c \in \mathcal{C}} y_c \log(p_c) + (1 - y_c) \log(1 - p_c),\end{aligned}\tag{7}$$

where C represents the number of classes within the dataset and BCE denotes the binary cross-entropy loss.

To further enhance the intra-class consistency of patch embeddings, we introduce an additional class-aware contrastive loss, \mathcal{L}_{PCE} , as described in Sec. 3.4. This loss pulls together high-confidence patches from the same class while pushing them away from low-confidence patches. It complements \mathcal{L}_{MCE} by improving patch-level discrimination and spatial consistency, which are critical under weak supervision. The overall loss function is defined as:

$$\mathcal{L}_{total} = \mathcal{L}_{MCE} + \lambda_{PCE} \sum_{c \in \mathcal{C}} \mathcal{L}_{PCE}^c,\tag{8}$$

where λ_{PCE} is a weighting hyperparameter controlling the influence of the contrastive term.

During the inference stage, we utilize the trained patch classifier to generate patch-level softmax class predictions Z . Following this, an interpolation algorithm is applied to Z to upsample and obtain pixel-level softmax predictions for the entire input image. Finally, an argmax operation is performed on the interpolated Z along the class dimension C to assign the class pseudo-label to each pixel, resulting in the final semantic segmentation output.

To elaborate further, during training our model focuses on reducing the discrepancy between the predicted probabilities and the true labels across all classes. The loss \mathcal{L}_{MCE} is computed by averaging the binary cross-entropy loss over the set of classes \mathcal{C} , ensuring that every class contributes equally regardless of its frequency in the dataset. This uniform treatment helps address any potential class imbalance and encourages the network to learn robust representations for both frequent and rare classes.

Meanwhile, the contrastive loss \mathcal{L}_{PCE} enforces compactness among high-confidence patch embeddings of the same category, acting as a structural regularizer that complements the global guidance from category clusters.

At inference time, the process shifts focus from training to generating meaningful predictions for new images. Initially, the trained patch classifier produces softmax outputs at the patch level, resulting in a prediction map Z . Since these predictions are at a lower resolution corresponding to the patches, an interpolation algorithm is applied to upscale Z to the original image resolution. This step ensures that the spatial details captured by the patch classifier are retained and properly represented in the final output. Finally, to convert these continuous softmax predictions into discrete class labels, an argmax operation is performed along the class dimension C . Each pixel is then assigned the label corresponding to the highest probability, yielding the final pseudo-label map for semantic segmentation. This complete pipeline enables our model to achieve precise segmentation results.

4. Experiments

In this section, we present our experimental settings and evaluation protocols. We compare our proposed method, Contrastive Prompt Clustering (CPC), with state-of-the-art weakly supervised semantic segmentation (WSSS) approaches on the PASCAL VOC 2012 Everingham et al. (2010) and MS COCO 2014 Lin et al. (2014) benchmarks. Finally, we perform ablation studies to validate the contributions of each component in our framework.

4.1. Experimental Settings

Datasets and Evaluation Metric. We evaluate the effectiveness of the proposed framework on two widely adopted benchmarks for weakly supervised semantic segmentation: PASCAL VOC 2012 Everingham et al. (2010) and MS COCO 2014 Lin et al. (2014). The PASCAL VOC 2012 dataset comprises 20 foreground object categories and one background class. Following standard

practice, we augment the original training set with additional annotations from the Semantic Boundaries Dataset (SBD) Hariharan et al. (2011), resulting in 10,582 training images annotated with image-level labels and 1,449 images reserved for validation. MS COCO 2014 provides a more challenging evaluation setting, containing 81 object categories with significant intra-class variation and complex scene compositions. In accordance with prior WSSS literature, we employ approximately 82,000 images with image-level supervision for training and 40,000 images from the validation set for performance evaluation.

For quantitative assessment, we adopt the standard mean Intersection over Union (mIoU) metric, which measures the average IoU across all semantic classes in the validation set. mIoU offers a balanced evaluation of both region-wise prediction accuracy and boundary localization, making it particularly suitable for benchmarking semantic segmentation performance under weak supervision.

Implementation Details. In our experiments, we utilize the ViT-B/16 model as the encoder, owing to its demonstrated ability to capture rich visual representations. Each image is resized to 384×384 during training Kolesnikov & Lampert (2016) to ensure consistent input resolution and is subsequently divided into 24×24 non-overlapping patches of size 16×16 . This patch-wise representation enables the transformer architecture to model both local and global contextual information through self-attention mechanisms.

The model is trained for 50 epochs with a batch size of 16 on two NVIDIA RTX 4090 GPUs. We adopt the Adam optimizer with an initial learning rate of 10^{-3} for the first two epochs, followed by a reduced learning rate of 10^{-4} for the remaining training duration. This two-stage schedule facilitates both rapid convergence and stable optimization.

During training, Top-K pooling with $k = 6$ is applied to the patch classifier outputs to aggregate the most salient patch-level activations, yielding image-level predictions supervised by the multi-label classification loss and query count of $R = 10$ is used to ensure stability in the LLM results. Additionally, we incorporate a patch contrastive learning module to improve intra-class feature compactness, where the contrastive loss is computed between high- and low-

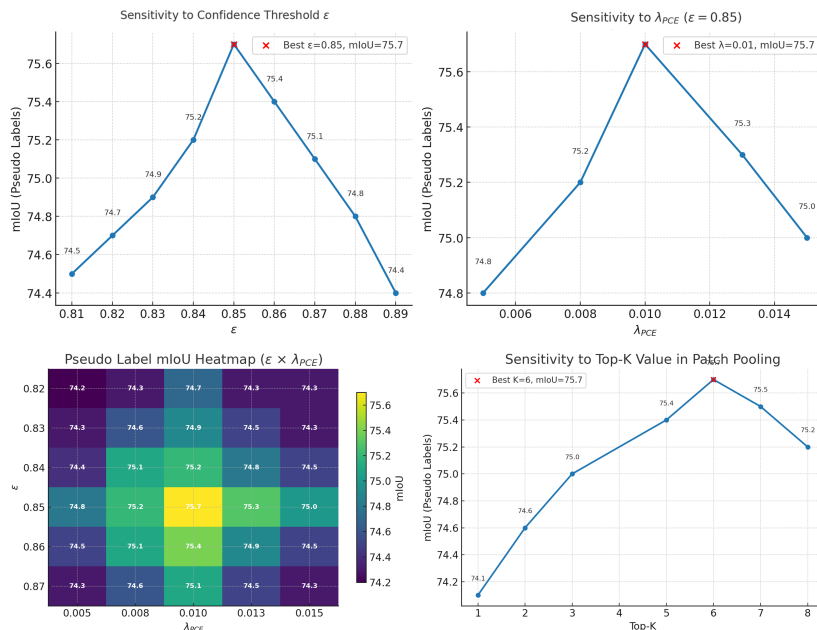


Figure 4: Qualitative visualization of segmentation results. Our CPC framework demonstrates clearer object boundaries and more accurate region predictions compared to baselines.

confidence patch embeddings for each class. Specifically, the high-confidence and low-confidence patches are selected using a predefined threshold $\epsilon = 0.85$. The final training objective combines the classification loss and the contrastive loss, with the latter weighted by a hyperparameter $\lambda_{PCE} = 0.01$.

For inference, input images are upsampled to 960×960 to generate high-resolution predictions. The patch classifier produces class probability maps, which are subsequently refined using Conditional Random Fields (CRF) Krähenbühl & Koltun (2011) to improve spatial coherence and boundary accuracy. These refined pseudo-labels are employed to supervise a DeepLab V2 Chen et al. (2018) segmentation model, which leverages atrous convolutions to capture multi-scale contextual dependencies, thereby producing the final dense semantic segmentation output.

Table 1: Pseudo Label Performance Comparison (mIoU) on PASCAL VOC 2012.

method	Pub.	Backbone	mIoU
AdvCAM Lee et al. (2022)	PAMI22	V2-RN101	69.9
SIPE Chen et al. (2022)	CVPR22	ResNet50	58.6
AFA Ru et al. (2022)	CVPR22	MiT-B1	66.0
ViT-PCM Dosovitskiy et al. (2020)	ECCV22	ViT-B/16	71.4
ToCo Ru et al. (2023)	CVPR23	ViT-B/16	72.2
USAGE Peng et al. (2023)	ICCV23	ResNet38	72.8
FPR Chen et al. (2023)	ICCV23	ResNet38	68.5
ToCo Ru et al. (2023)	CVPR23	ViT-B/16	70.5
SFC Zhao et al. (2024)	AAAI24	ViT-B/16	73.7
APC Wu et al. (2025b)	EAAI25	ViT-B/16	74.6
CPC	Ours	ViT-B/16	75.7

4.2. Comparison with State-of-the-arts

Pseudo Label Performance Comparison . The proposed CPC framework effectively exploits the latent semantic correlations among visually similar categories, enabling the model to better disambiguate closely related classes under weak supervision. By introducing prompt-guided category clusters, the model captures shared feature structures that are often overlooked in conventional approaches. This facilitates the learning of more discriminative and semantically aware patch representations, ultimately leading to improved pseudo-label quality.

In addition to the inter-class clustering, our framework integrates a patch-level contrastive loss to further enhance intra-class consistency, which contributes to more coherent and robust pixel-level predictions. Together, these components allow the model to more accurately distinguish between ambiguous regions and reduce misclassification errors caused by overlapping semantics. As shown in Tab. 1, our method achieves superior mIoU performance compared to a range of recent state-of-the-art methods, including both convolution-based and

transformer-based backbones. Notably, CPC outperforms strong baselines such as ToCo Ru et al. (2023) and SFC Zhao et al. (2024), demonstrating the effectiveness of our dual-level learning strategy in producing high-quality pseudo labels.

Table 2: Semantic Segmentation Performance Comparison (mIoU) on PASCAL VOC 2012.

Model	Pub.	Backbone	Val
USAGE Peng et al. (2023)	ICCV23	ResNet38	71.9
SAS Kim et al. (2023)	AAAI23	ViT-B/16	69.5
MCTformer Xu et al. (2022)	CVPR22	DeiT-S	61.7
SIPE Chen et al. (2022)	CVPR22	ResNet50	58.6
ViT-PCM Dosovitskiy et al. (2020)	ECCV22	ViT-B/16	69.3
AFA Ru et al. (2022)	CVPR22	MiT-B1	63.8
ToCo Ru et al. (2023)	CVPR23	ViT-B/16	70.5
TSCD Xu et al. (2023)	AAAI23	MiT-B1	67.3
FPR Chen et al. (2023)	ICCV23	ResNet38	70.0
SFC Zhao et al. (2024)	AAAI24	ViT-B/16	71.2
IACD Wu et al. (2024a)	ICASSP24	ViT-B/16	71.4
APC Wu et al. (2025b)	EAAI25	ViT-B/16	72.3
CPC	Ours	ViT-B/16	73.4

Semantic Segmentation Results. To evaluate the effectiveness of our proposed pseudo-label generation strategy, we adopt DeepLab V2 Chen et al. (2018) as the segmentation backbone and train it using the pseudo labels generated by our CPC framework. We report semantic segmentation performance on the PASCAL VOC 2012 validation set and compare it with recent state-of-the-art WSSS approaches, as presented in Tab. 2. Our CPC framework yields superior segmentation performance, achieving an mIoU of 72.2% and outperforming prior transformer-based methods such as ToCo Ru et al. (2023), SFC Zhao et al. (2024), and IACD Wu et al. (2024a). These results confirm the advantage of

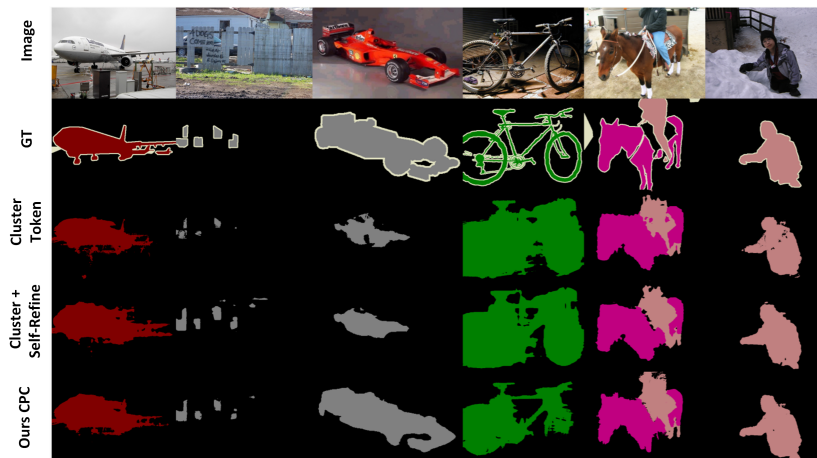


Figure 5: Qualitative visualization of segmentation results. Our CPC framework demonstrates clearer object boundaries and more accurate region predictions compared to baselines.

combining inter-class category clustering with intra-class contrastive learning for generating high-quality pseudo labels. The enhanced quality of pseudo labels leads to clearer delineation of complex object structures and reduced confusion between visually similar classes.

Visualization of Result. To further assess the effectiveness of our method, we present qualitative segmentation results in Fig. 5. Compared to existing state-of-the-art approaches, our CPC framework produces significantly more accurate and coherent segmentation outputs, particularly in regions characterized by fine-grained object boundaries and semantic overlaps. As illustrated, CPC effectively mitigates common segmentation errors such as over-smoothing and misclassification, resulting in clearer object contours and improved region integrity. These observations align well with the quantitative improvements and confirm the model’s enhanced ability to capture precise semantic structures.

In addition, we provide heatmap visualizations in Fig. 6 to interpret the model’s confidence across spatial locations. In these maps, pixel intensity reflects the predicted probability of belonging to the target class, with yellow indicating higher confidence. The results show that our model exhibits strong activations in object centers and smooth gradients toward object boundaries, indicating

Table 3: Semantic Segmentation Performance Comparison (mIoU) on MS COCO 2014.

Model	Pub.	Backbone	mIoU (%)
MCTformer Xu et al. (2022)	CVPR22	Resnet38	42.0
ViT-PCM Dosovitskiy et al. (2020)	ECCV22	ViT-B/16	45.0
SIPE Chen et al. (2022)	CVPR22	Resnet38	43.6
TSCD Xu et al. (2023)	AAAI23	MiT-B1	40.1
SAS Kim et al. (2023)	AAAI23	ViT-B/16	44.5
FPR Chen et al. (2023)	ICCV23	ResNet38	43.9
ToCo Ru et al. (2023)	CVPR23	ViT-B	42.3
SFC Zhao et al. (2024)	AAAI24	ViT-B/16	44.6
IACD Wu et al. (2024a)	ICASSP24	ViT-B/16	44.3
PGSD Hao et al. (2024)	TCSVT24	ViT-B/16	43.9
APC Wu et al. (2025b)	EAAI25	ViT-B/16	45.7
CPC	Ours	ViT-B/16	46.7

a well-calibrated spatial awareness. Notably, CPC yields sharper and more localized class-specific activations compared to prior methods, highlighting its superior ability to preserve semantic focus and reduce ambiguity at transition regions. These findings further validate that our approach enhances both object localization and semantic consistency across diverse visual scenes.

4.3. Ablation Studies

Table 4: Ablation studies on the impact of Self Refine, cluster token, and contrastive learning on PASCAL VOC 2012 Val

Original Framework	Cluster Token	Self Refine	Contrastive Learning	mIoU
✓				68.6%
✓	✓			71.1%
✓	✓	✓		72.2%
✓	✓	✓	✓	73.4%

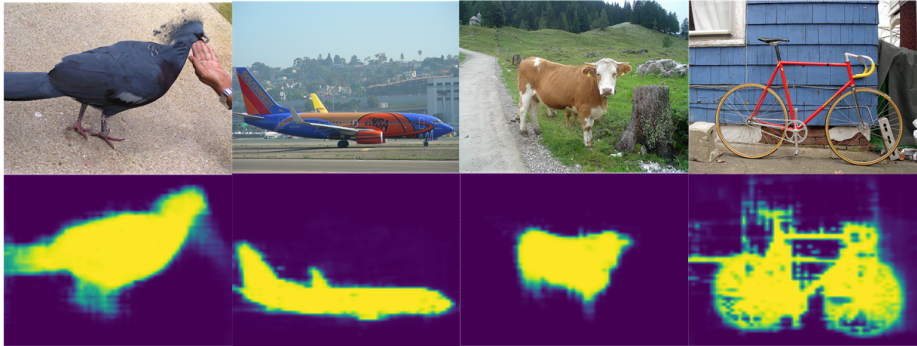


Figure 6: Visualization of class-specific activation heatmaps. Yellow pixels indicate higher predicted probability for the target class, highlighting the model’s spatial confidence.

To validate the contribution of each core component in our framework, we conduct ablation studies on the PASCAL VOC 2012 validation set. As summarized in Tab. 4, we evaluate the individual and combined effects of Self Refine, cluster token, and contrastive learning. Starting from a baseline ViT that uses only patch tokens, we first add the cluster token derived from GPT-generated category groupings. This token captures high-level semantic relations across categories and improves the model’s ability to reason about inter-class similarity, resulting in a +2.5% mIoU gain. Next, we introduce the Self Refine mechanism, which performs multiple LLM queries followed by refinement, providing a more stable and semantically consistent cluster representation. This contributes an additional +1.1% improvement. Finally, we incorporate a patch-level contrastive learning module that enforces intra-class consistency and encourages better separation of uncertain regions, leading to the highest mIoU of 73.4%.

To evaluate the effect of query count R in our Self-Refine clustering module, we conduct an ablation study focused on how different values of R influence the stability of generated category clusters and the final segmentation performance. For each small R (e.g., 2 or 6), we run the entire pipeline three times with independently sampled clusters and report the average mIoU and standard deviation. For large R (e.g., 10), we observe consistent cluster outputs after majority voting and report the mIoU from a single run. As shown in Tab. 5,

increasing R improves cluster stability and leads to better and more reliable segmentation results.

Table 5: Impact of the number of LLM queries R on cluster stability and Semantic Segmentation Performance on PASCAL VOC 2012

R	Cluster Stability	mIoU (avg \pm std)	Note
2	✗ Unstable	73.0 \pm 0.2	Avg of 3 runs
6	✗ Occasionally Stable	73.1 \pm 0.1	Avg of 3 runs
10	✓ Stable	73.4	Voted cluster, 1 run

These results demonstrate that a sufficiently large query count R is crucial for ensuring semantically stable cluster assignments and reproducible segmentation performance. While smaller R values can sometimes yield reasonable results, their non-deterministic nature introduces performance fluctuations and undermines robustness. Our final model adopts $R = 10$ to balance cluster quality and computational efficiency.

5. Conclusion

We propose CPC, a novel framework for WSSS. Unlike prior methods that process each category independently, CPC leverages LLM-generated category clusters to model inter-class semantic relationships. These clusters are encoded as learnable tokens and injected into the ViT backbone to enhance the model’s ability to distinguish semantically similar classes. In addition, we introduce a class-aware patch contrastive loss to improve intra-class feature consistency. Combined, these components significantly improve pseudo-label quality and achieve state-of-the-art performance using only image-level supervision.

Beyond individual module effectiveness, our framework highlights the synergy between high-level semantic reasoning from language models and fine-grained visual discrimination through contrastive learning. This hierarchical design enables the model to simultaneously leverage global category relationships and local feature consistency, addressing long-standing challenges in WSSS such as

semantic ambiguity and over-smoothing. Extensive experiments on PASCAL VOC and MS COCO demonstrate the robustness and generality of our method across diverse datasets. We believe CPC provides a promising foundation for future research at the intersection of vision and language in weakly supervised learning scenarios.

6. Acknowledgements

This work was supported by the National Natural Science Foundation of China (No. 62471405, 62331003, 62301451), Suzhou Basic Research Program (SYG202316) and XJTLU REF-22-01-010, XJTLU AI University Research Centre, Jiangsu Province Engineering Research Centre of Data Science and Cognitive Computation at XJTLU and SIP AI innovation platform (YZCXPT2022103).

References

- Ahn, J., & Kwak, S. (2018). Learning pixel-level semantic affinity with image-level supervision for weakly supervised semantic segmentation. In *Proc. IEEE Conf. Comput. Vis. Pattern Recog.* (pp. 4981–4990).
- Brown, T., Mann, B., Ryder, N., Subbiah, M., Kaplan, J. D., Dhariwal, P., Neelakantan, A., Shyam, P., Sastry, G., Askell, A. et al. (2020). Language models are few-shot learners, . *33*, 1877–1901.
- Cao, Z., & Zhang, J. (2023). Gradient-coupled cross-patch attention map for weakly supervised semantic segmentation. *Neurocomputing*, *535*, 83–96.
- Chang, Y.-T., Wang, Q., Hung, W.-C., Piramuthu, R., Tsai, Y.-H., & Yang, M.-H. (2020). Weakly-supervised semantic segmentation via sub-category exploration. In *Proc. IEEE Conf. Comput. Vis. Pattern Recog.* (pp. 8991–9000).
- Chen, H., Ren, J., Gu, J., Wu, H., Lu, X., Cai, H., & Zhu, L. (). Snow removal in video: A new dataset and a novel method. in 2023 ieee. In *CVF International Conference on Computer Vision (ICCV)* (pp. 13165–13176).

- Chen, L., Lei, C., Li, R., Li, S., Zhang, Z., & Zhang, L. (2023). Fpr: False positive rectification for weakly supervised semantic segmentation. In *Proc. IEEE Int. Conf. Comput. Vis.* (pp. 1108–1118).
- Chen, L.-C., Zhu, Y., Papandreou, G., Schroff, F., & Adam, H. (2018). Encoder-decoder with atrous separable convolution for semantic image segmentation. In *Eur. Conf. Comput. Vis.* (pp. 801–818).
- Chen, Q., Chen, Y., Huang, Y., Xie, X., & Yang, L. (2024). Region-based online selective examination for weakly supervised semantic segmentation. *Information Fusion*, 107, 102311.
- Chen, Q., Yang, L., Lai, J.-H., & Xie, X. (2022). Self-supervised image-specific prototype exploration for weakly supervised semantic segmentation. In *Proc. IEEE Conf. Comput. Vis. Pattern Recog.* (pp. 4288–4298).
- Dosovitskiy, A., Beyer, L., Kolesnikov, A., Weissenborn, D., Zhai, X., Unterthiner, T., Dehghani, M., Minderer, M., Heigold, G., Gelly, S. et al. (2020). An image is worth 16x16 words: Transformers for image recognition at scale. *arXiv preprint arXiv:2010.11929*, .
- Du, Y., Fu, Z., Liu, Q., & Wang, Y. (2022). Weakly supervised semantic segmentation by pixel-to-prototype contrast. In *Proc. IEEE Conf. Comput. Vis. Pattern Recog.* (pp. 4320–4329).
- Everingham, M., Van Gool, L., Williams, C. K., Winn, J., & Zisserman, A. (2010). The pascal visual object classes (VOC) challenge. *Int. J. Comput. Vis.*, 88, 303–338.
- Fang, T., Zhang, T., Wong, D. F., Jin, K., Zhang, L., Zhang, Q., Li, T., Hou, J., & Chao, L. S. (2025). Llmcl-gec: Advancing grammatical error correction with llm-driven curriculum learning. *Expert Systems with Applications*, .
- Guo, X., Chen, X., Luo, S., Wang, S., & Pun, C.-M. (2024). Dual-hybrid attention network for specular highlight removal. In *ACM MM* (pp. 10173–10181).

- Hao, X., Jiang, X., Ni, W., Tan, W., & Yan, B. (2024). Prompt-guided semantic-aware distillation for weakly supervised incremental semantic segmentation. *IEEE Transactions on Circuits and Systems for Video Technology*, .
- Hariharan, B., Arbeláez, P., Bourdev, L., Maji, S., & Malik, J. (2011). Semantic contours from inverse detectors. In *Proc. IEEE Int. Conf. Comput. Vis.* (pp. 991–998).
- Jiang, J., Zhao, M., Shen, Z., & Yan, D.-M. (2022). Edsf: Fast and accurate ellipse detection via disjoint-set forest, . (pp. 1–6).
- Jiang, P.-T., Hou, Q., Cao, Y., Cheng, M.-M., Wei, Y., & Xiong, H.-K. (2019). Integral object mining via online attention accumulation. In *Proceedings of the IEEE/CVF international conference on computer vision* (pp. 2070–2079).
- Jin, K., Wang, Y., Santos, L., Fang, T., Yang, X., & Im, S. K. (2025). Sscm: Self-supervised critical model for reducing hallucinations in chinese financial text generation. In *IEEE Int. Conf. Acoust. Speech Signal Process.*.
- Kim, S., Park, D., & Shim, B. (2023). Semantic-aware superpixel for weakly supervised semantic segmentation. In *AAAI Conf. Artif. Intell.* (pp. 1142–1150). volume 37.
- Kolesnikov, A., & Lampert, C. H. (2016). Seed, expand and constrain: Three principles for weakly-supervised image segmentation. In *Eur. Conf. Comput. Vis.* (pp. 695–711).
- Krähenbühl, P., & Koltun, V. (2011). Efficient inference in fully connected crfs with gaussian edge potentials. In *Int. Conf. Neur. Info. Process. Sys.*. volume 24.
- Kweon, H., & Yoon, K.-J. (2024). From sam to cams: Exploring segment anything model for weakly supervised semantic segmentation. In *Proceedings of the IEEE/CVF Conference on Computer Vision and Pattern Recognition* (pp. 19499–19509).

- Lee, J., Kim, E., Mok, J., & Yoon, S. (2022). Anti-adversarially manipulated attributions for weakly supervised semantic segmentation and object localization. *IEEE Trans. Pattern Anal. Mach. Intell.*, .
- Lee, S., Lee, M., Lee, J., & Shim, H. (2021). Railroad is not a train: Saliency as pseudo-pixel supervision for weakly supervised semantic segmentation. In *Proc. IEEE Conf. Comput. Vis. Pattern Recog.* (pp. 5495–5505).
- Li, M., Sun, H., Lei, Y., Zhang, X., Dong, Y., Zhou, Y., Li, Z., & Chen, X. (2024). High-fidelity document stain removal via a large-scale real-world dataset and a memory-augmented transformer. In *WACV*.
- Li, X. L., & Liang, P. (2021). Prefix-tuning: Optimizing continuous prompts for generation. *arXiv preprint arXiv:2101.00190*, .
- Li, Z., Chen, X., Pun, C.-M., & Cun, X. (2023). High-resolution document shadow removal via a large-scale real-world dataset and a frequency-aware shadow erasing net. In *ICCV* (pp. 12449–12458).
- Lin, T.-Y., Maire, M., Belongie, S., Hays, J., Perona, P., Ramanan, D., Dollár, P., & Zitnick, C. L. (2014). Microsoft coco: Common objects in context. In *Eur. Conf. Comput. Vis.* (pp. 740–755). Springer.
- Liu, J., Liu, Y., Shang, F., Liu, H., Liu, J., & Feng, W. (2025). Improving generalization in federated learning with highly heterogeneous data via momentum-based stochastic controlled weight averaging. In *Forty-second International Conference on Machine Learning*.
- Liu, J., Shang, F., Liu, Y., Liu, H., Li, Y., & Gong, Y. (2024). Fedbcgd: Communication-efficient accelerated block coordinate gradient descent for federated learning. In *Proceedings of the 32nd ACM International Conference on Multimedia* (pp. 2955–2963).
- Liu, X., Zheng, Y., Du, Z., Ding, M., Qian, Y., Yang, Z., & Tang, J. (2023). Gpt understands, too. *AI Open*, .

- Luo, Y., Xu, C., Liu, Y., Liu, W., Zheng, S., & Bian, J. (2022). Learning differential operators for interpretable time series modeling. In *Proceedings of the 28th ACM SIGKDD Conference on Knowledge Discovery and Data Mining* (pp. 1192–1201).
- Madaan, A., Tandon, N., Gupta, P., Hallinan, S., Gao, L., Wiegrefe, S., Alon, U., Dziri, N., Prabhunoye, S., Yang, Y. et al. (2024). Self-refine: Iterative refinement with self-feedback. *Advances in Neural Information Processing Systems*, 36.
- Peng, Z., Wang, G., Xie, L., Jiang, D., Shen, W., & Tian, Q. (2023). Usage: A unified seed area generation paradigm for weakly supervised semantic segmentation. In *Proc. IEEE Int. Conf. Comput. Vis.* (pp. 624–634).
- Raffel, C., Shazeer, N., Roberts, A., Lee, K., Narang, S., Matena, M., Zhou, Y., Li, W., & Liu, P. J. (2020). Exploring the limits of transfer learning with a unified text-to-text transformer, . 21, 5485–5551.
- Rossetti, S., Zappia, D., Sanzari, M., Schaerf, M., & Pirri, F. (2022). Max pooling with vision transformers reconciles class and shape in weakly supervised semantic segmentation. In *European conference on computer vision* (pp. 446–463). Springer.
- Ru, L., Zhan, Y., Yu, B., & Du, B. (2022). Learning affinity from attention: End-to-end weakly-supervised semantic segmentation with transformers. In *Proc. IEEE Conf. Comput. Vis. Pattern Recog.* (pp. 16846–16855).
- Ru, L., Zheng, H., Zhan, Y., & Du, B. (2023). Token contrast for weakly-supervised semantic segmentation. In *Proc. IEEE Conf. Comput. Vis. Pattern Recog.* (pp. 3093–3102).
- Shin, T., Razeghi, Y., Logan IV, R. L., Wallace, E., & Singh, S. (2020). Autoprompt: Eliciting knowledge from language models with automatically generated prompts. *arXiv preprint arXiv:2010.15980*, .

- Sun, G., Wang, W., Dai, J., & Van Gool, L. (2020). Mining cross-image semantics for weakly supervised semantic segmentation. In *Computer Vision–ECCV 2020: 16th European Conference, Glasgow, UK, August 23–28, 2020, Proceedings, Part II 16* (pp. 347–365). Springer.
- Wei, Y., Feng, J., Liang, X., Cheng, M.-M., Zhao, Y., & Yan, S. (2017). Object region mining with adversarial erasing: A simple classification to semantic segmentation approach. In *Proc. IEEE Conf. Comput. Vis. Pattern Recog.* (pp. 1568–1576).
- Wu, W., Dai, T., Chen, Z., Huang, X., Ma, F., & Xiao, J. (2025a). Generative prompt controlled diffusion for weakly supervised semantic segmentation. *Neurocomputing*, (p. 130103).
- Wu, W., Dai, T., Chen, Z., Huang, X., Xiao, J., Ma, F., & Ouyang, R. (2025b). Adaptive patch contrast for weakly supervised semantic segmentation. *Engineering Applications of Artificial Intelligence*, 139, 109626.
- Wu, W., Dai, T., Huang, X., Ma, F., & Xiao, J. (2024a). Image augmentation with controlled diffusion for weakly-supervised semantic segmentation. In *IEEE Int. Conf. Acoust. Speech Signal Process.* (pp. 6175–6179). IEEE.
- Wu, W., Dai, T., Huang, X., Ma, F., & Xiao, J. (2024b). Top-k pooling with patch contrastive learning for weakly-supervised semantic segmentation. In *2024 IEEE International Conference on Systems, Man, and Cybernetics (SMC)* (pp. 5270–5275). IEEE.
- Wu, W., Qiu, X., Song, S., Chen, Z., Huang, X., Ma, F., & Xiao, J. (2024c). Image augmentation agent for weakly supervised semantic segmentation. *arXiv preprint arXiv:2412.20439*, .
- Wu, W., Qiu, X., Song, S., Chen, Z., Huang, X., Ma, F., & Xiao, J. (2025c). Prompt categories cluster for weakly supervised semantic segmentation. In *Proceedings of the Computer Vision and Pattern Recognition Conference* (pp. 3198–3207).

- Xie, R., Chen, J., Jiang, L., Xiao, R., Pan, Y., & Cai, Y. (2024a). Accurate explanation model for image classifiers using class association embedding. In *2024 IEEE 40th International Conference on Data Engineering (ICDE)* (pp. 2271–2284). IEEE.
- Xie, R., Jiang, L., He, X., Pan, Y., & Cai, Y. (2024b). A weakly supervised and globally explainable learning framework for brain tumor segmentation. In *2024 IEEE International Conference on Multimedia and Expo (ICME)* (pp. 1–6). IEEE.
- Xu, C., Qin, T., Wang, G., & Liu, T.-Y. (2019). Polygon-net: A general framework for jointly boosting multiple unsupervised neural machine translation models. In *IJCAI* (pp. 5320–5326).
- Xu, L., Ouyang, W., Bennamoun, M., Boussaid, F., & Xu, D. (2022). Multi-class token transformer for weakly supervised semantic segmentation. In *Proc. IEEE Conf. Comput. Vis. Pattern Recog.* (pp. 4310–4319).
- Xu, R., Wang, C., Sun, J., Xu, S., Meng, W., & Zhang, X. (2023). Self correspondence distillation for end-to-end weakly-supervised semantic segmentation. In *AAAI Conf. Artif. Intell.* (pp. 3045–3053). volume 37.
- Xue, Z., Guo, D., Chen, D., Zhang, Y., Lin, X., & Liu, S. (2025). Weakly supervised semantic segmentation via multi-type semantic affinity learning. *Knowledge-Based Systems*, (p. 113933).
- Yaganapu, A., & Kang, M. (2024). Multi-layered self-attention mechanism for weakly supervised semantic segmentation. *Computer Vision and Image Understanding*, 239, 103886.
- Yao, Y., Chen, T., Xie, G.-S., Zhang, C., Shen, F., Wu, Q., Tang, Z., & Zhang, J. (2021). Non-salient region object mining for weakly supervised semantic segmentation. In *Proc. IEEE Conf. Comput. Vis. Pattern Recog.* (pp. 2623–2632).

- Yin, J., Peng, N., Chen, Y., Zheng, Z., Gu, Y., & Zhou, J. (2024). Class-level multiple distributions representation are necessary for semantic segmentation. In *International Conference on Database Systems for Advanced Applications* (pp. 340–351). Springer.
- Yin, J., Zheng, Z., Pan, Y., Gu, Y., & Chen, Y. (2023). Semi-supervised semantic segmentation with multi-reliability and multi-level feature augmentation. *Expert Systems with Applications*, 233, 120973.
- Zhang, H., Xu, C., Zhang, Y.-F., Zhang, Z., Wang, L., & Bian, J. (2025). Timeraf: Retrieval-augmented foundation model for zero-shot time series forecasting. *IEEE Transactions on Knowledge and Data Engineering*, .
- Zhang, R., Hu, X., Li, B., Huang, S., Deng, H., Qiao, Y., Gao, P., & Li, H. (2023). Prompt, generate, then cache: Cascade of foundation models makes strong few-shot learners. In *Proc. IEEE Conf. Comput. Vis. Pattern Recog.* (pp. 15211–15222).
- Zhao, X., Tang, F., Wang, X., & Xiao, J. (2024). Sfc: Shared feature calibration in weakly supervised semantic segmentation. In *AAAI Conf. Artif. Intell.* (pp. 7525–7533). volume 38.
- Zou, X., Yin, D., Zhong, Q., Yang, H., Yang, Z., & Tang, J. (2021). Controllable generation from pre-trained language models via inverse prompting. In *Proceedings of the 27th ACM SIGKDD Conference on Knowledge Discovery & Data Mining* (pp. 2450–2460).